Royal Netherlands Institute for Sea Research

This is a postprint of:

Bordois, L., Auclair, F., Paci, A., Dossmann, Y., Gerkema, T. & Nguyen, C. (2016). Tidal energy redistribution among vertical modes in a fluid with a mid-depth pycnocline. *Physics of Fluids*, 28(10), 101701.

Published version: dx.doi.org/10.1063/1.4964759

Link NIOZ Repository: www.vliz.be/nl/imis?module=ref&refid=282183

[Article begins on next page]

The NIOZ Repository gives free access to the digital collection of the work of the Royal Netherlands Institute for Sea Research. This archive is managed according to the principles of the Open Access Movement, and the Open Archive Initiative. Each publication should be cited to its original source - please use the reference as presented.
When using parts of, or whole publications in your own work, permission from the author(s) or copyright holder(s) is always needed.

AIP Publishing

This manuscript was accepted by Phys. Fluids. Click here to see the version of record.

Tidal energy redistribution among vertical modes in a fluid with a mid-depth pycnocline

Bordois L.[1,2], Auclair F. [2], Paci A.[1], Dossmann Y.[3], Gerkema T.[4], Nguyen C. [2]

[1] *CNRM, UMR3589 METEO-FRANCE and CNRS, 42 avenue Gaspard Coriolis, 31057 Toulouse Cedex 01, France*
[2] *Laboratoire d'Aérologie, 14 avenue Edouard Belin, 31400 Toulouse, France*
[3] *Laboratoire de Physique, Ecole Normale Supérieure, 46 allée d'Italie, 69007 Lyon, France*
[4] *NIOZ Royal Netherlands Institute for Sea Research, Department of Estuarine and Delta Systems (EDS), and Utrecht University, P.O. Box 140, 4400 AC Yerseke, The Netherlands*

We modeled internal tide generation above a high sinusoidal ridge in a fluid with a mid-depth pycnocline and developed an original method to quantify internal tide vertical mode amplitude in 2D-vertical simulations. Since lowest modes can propagate over considerable distances, while high modes are more likely to dissipate locally, estimating the tidal energy distribution among vertical modes is necessary to investigate the spatial redistribution of the tidal energy. Our numerical approach allows expansion and verification of previous analytical studies over a larger range of configurations. The tidal energy distribution among vertical modes is shown here to be dependent on the topographic resonance criterion and the topographic blocking parameter.

Internal tides are ubiquitous and play an essential role in the oceans. They are involved in the Meridional Overturning Circulation energy balance (Munk and Wunsch[1]; Egbert and Ray[2]; Wunsch and Ferrari[3]). The current debate about the relative importance of the mechanical and thermodynamical energy sources (Ferrari and Wunsch[4]) induces a need for an evaluation of the energy transfers and of the energy redistribution in the ocean. In an ocean of finite and constant depth, the internal waves (IWs) field can be decomposed into a linear superposition of vertical normal modes, which are determined through solving a Sturm-Liouville eigenvalue problem depending only on the tidal frequency ω and on the buoyancy frequency profile $N(z)$. The lowest modes can propagate over a considerable distance, contributing eventually to a remote mixing, while high modes are more likely to dissipate locally, near the generation site. Hence, the energy distribution among the vertical modes needs to be determined to investigate precisely the spatial redistribution of the tidal energy. The energy distribution among these vertical modes is highly variable in the oceans depending on the generation site. Previous analytical studies[5–7] have highlighted a strong relationship between vertical mode amplitudes and the topography shape of the generation site (height, width, slope). These analytical approaches rely on strong assumptions: linear approximation (weak wave amplitude limit), infinitesimal topography or subcritical topography, "propagative" environment ($\omega<N(z)$ limit). In this letter, following the line of research of these analytical theories, we estimate the tidal energy distribution among vertical modes in direct numerical simulations. The numerical approach allows us to study a wider range of configurations in particular stratification profiles with non-propagative layers and high and steep topographies. Numerical simulations of primary generation of IWs ("primary" as defined by Dossmann *et al.*[8], in opposition to secondary or local generation) are analyzed to describe the tidal energy redistribution among vertical modes inside the pycnocline layer near high and abrupt oceanic ridges.

Two-dimensional (2D) direct numerical simulations in a vertical plane are performed using the free-surface nonhydrostatic and non-Boussinesq version of the regional oceanic

ACCEPTED MANUSCRIPT

AIP Publishing

This manuscript was accepted by Phys. Fluids. Click here to see the version of record.

circulation model SNH described in Auclair *et al.*[9,10]. This version uses an original three-mode time-splitting technique between barotropic (Δt_e), baroclinic (Δt_i) and non-Boussinesq (Δt_{NBQ}) motions to deal with non-hydrostatic flows and acoustic waves which are explicitly simulated. Previously, similar simulations of internal tide generation performed with the nonhydrostatic version of SNH have been compared and validated by laboratory experiments[8,11,12]. A schematic of the numerical configuration, incorporating a plot of the initial stratification profile, is presented in figure 1. Table 1 summarizes the parameters of this configuration. We applied periodic horizontal boundary conditions, free surface boundary and no-slip condition at the bottom of the domain. Molecular values of the kinematic viscosity (ν = 10^{-6} m^2/s) and of the density diffusivity (K_ρ= 10^{-7} m^2/s) are used, without any turbulence closure scheme. Numerical dissipation is provided by the upstream advection scheme. The level of dissipation of the upstream scheme has been reduced by a multiplicative coefficient of 0.01: upstream advection scheme = centered scheme + 0.01 · diffusive scheme.

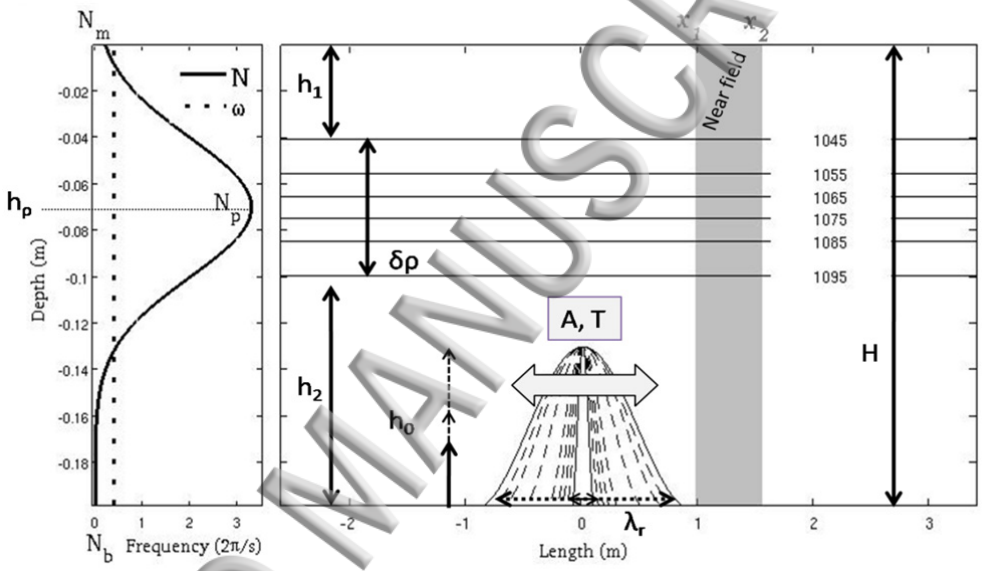

FIG. 1. Left: initial stratification profile (solid line). The dotted line indicates the IW forcing frequency. Right: Numerical configuration sketch. Density contours: 6 isopycnal lines at t =0. The density difference between two isopycnals is $d\rho$ = 10 kg/m ^{3}. Indicated physical parameters are defined in Table 1.

The topography is represented by a high sinusoidal ridge whose shape is given by:

$$h(x_m) = \begin{cases} \frac{1}{2} h_0 \left(1 + cos\, 2\pi \frac{x_m}{2l}\right) & for\ x \in [-l, l\,] \\ 0 & for\ x < -\,l\ and\ x > l \end{cases} \quad (1)$$

where h_0 and l are the height and the half-width of the ridge. At t=0, the ridge is centered at 0 m. Various shapes of the ridge (λ_r, h_0) are explored (table 1) to study the impact of the topography shape on the multimodal structure of the IWs field. Tidal forcing is performed through the oscillation of the ridge[13]. The following ridge displacement is given by $x_m(t) = A\left[\cos\left(\frac{2\pi}{T}t - \pi\right) - 1\right]$, where $x_m(t)$ is the horizontal position of the center of the ridge, (A, T) are the forcing amplitude and period. Gerkema and Zimmerman[14] have shown that a tidal motion over a ridge is equivalent to an oscillating topography if the nonlinearity parameter $\varepsilon = \frac{Ah_0}{\lambda_r H}$ and the topography parameter $\varepsilon_b = \frac{h_0}{l}$ are small, with H the fluid depth. The nonlinearity parameter is linked to the conversion efficiency from horizontal to vertical displacement by the ridge. In our configurations, the nonlinearity parameter is small (ε <0.01) whereas the topography parameter is only smaller than one ($\varepsilon_b \leq 0.35$), hence some

ACCEPTED MANUSCRIPT

AIP Publishing

This manuscript was accepted by Phys. Fluids. Click here to see the version of record.

divergences may appear between the present case and the real tidal forcing case. The Brunt-Väisälä frequency profile, $N(z)$, (figure 1-left) is inspired by oceanic observations and is the same as the one used in Grisouard *et al.*[15]:

$$N^2(z) = \frac{2}{\sqrt{\pi}} g \frac{\Delta\rho}{\delta\rho} exp\left[-\left(\frac{z+h_p}{\delta\rho/2}\right)^2\right] + \begin{cases} {N_b}^2 \; for \; -H \le z < -h_p \\ 0 \; for \; -h_p \le z \le 0 \end{cases} \quad (2)$$

with g the acceleration of gravity.

The forcing frequency ω is chosen such that $\{N_b, N_m\} < \omega < N_p$ with $N_b = N(z=0)$ and $N_m = N(z=-h_P)$ (figure 1). Hence, the pycnocline N_P layer is a waveguide supporting propagating internal waves, with evanescent decay taking place in the bottom N_b and in the mixing N_m layer. This particular stratification profile with non-propagative bottom and surface layers deviates from one of the basic assumptions of analytical theories.

	Designation	Name	Value
Fluid	Kinematic viscosity	ν (m^2/s)	2×10^{-6}
	Density diffusivity	K_ρ (m^2/s)	10^{-7}
	Coriolis force	f (rad/s)	0
	Total depth	H (m)	0.2
	Domain length	L (m)	20
Stratification	Pycnocline depth	h_ρ (m)	0.07
	Pycnocline thickness	$\delta\rho$ (m)	0.06
	Density jump	$\Delta\rho$ (kg/m^3)	60
	Upper and Bottom layer density	$\rho_{1,2}$ (kg/m^3)	$\begin{cases}1040\\1100\end{cases}$
	Bottom layer stratification	N_b (s^{-1})	0.001
	Upper and bottom layer depth	$h_{1,2} = \begin{cases} h_\rho - \frac{\delta\rho}{2} \\ H - h_\rho - \frac{\delta\rho}{2} \end{cases}$ (m)	$\begin{cases}0.04\\0.1\end{cases}$
Forcing	Ridge height	h_0 (m)	[0.03,0.07]
	Ridge width	λ_r(m)	[0.2,1.9]
	Topographic blocking Degree	$B = h_0/h_2$	[0.3,0.7]
	Forcing amplitude	A (m)	0.006
	Forcing period	T (s)	16
IW	Nonlinearity parameter	$\varepsilon = \frac{Ah_0}{\lambda_r H}$	[0.0011,0.01] < 0.018
Numerical	Spatial resolution	Δ (mm)	≈ 2
	Sigma level number	N_σ	100
	Internal time step and ratio with external and non-Boussinesq time step	Δt_i (s) / $\Delta t_i/\Delta t_e$ / $\Delta t_{NBQ}/\Delta t_e$	2.10^{-3} / 100 / 4

TABLE 1 –Numerical and physical parameters of the configuration

We developed an original method to quantify the vertical mode amplitude in the numerical simulations. The classical Sturm-Liouville eigenvalue problem of vertical mode

ACCEPTED MANUSCRIPT

AIP Publishing

This manuscript was accepted by Phys. Fluids. Click here to see the version of record.

decomposition is numerically resolved for the initial buoyancy profile $N(z)$ above the flat bottom (outside the generation site) for a non-rotating case with the same approach as Gerkema and Zimmerman[7]:

$$\frac{\partial^2 W_n(z)}{\partial z^2} + {k_{x,n}}^2 \left(\frac{N^2(z) - \omega^2}{\omega^2} \right) W_n(z) = 0 \qquad (3)$$

where W_n, k_n, are respectively the vertical modal structure and the wavenumber; ω is the wave frequency and $n \in N^*$ is the mode number. The velocity of a vertical mode n is then defined as $c_n = \frac{2\pi}{T k_n}$. Our study is limited to the first four modes (n = 1…4). We used these analytical vertical mode structures $W_n(z)$, as a base projection for the simulations. Such modal computation is based on linear approximation. Thus, to optimize the agreement between this theoretical approach and modal vertical structure in the simulations, we first study the linear regime of internal tides. Dossmann *et al.*[8] show that non linear effects and internal solitary wave formations appear in a clear way for a nonlinearity parameter, ε, of at least $\varepsilon_0 = 0.018$. Hence, in these simulations, all the regimes are supposed to be linear: $\varepsilon < \varepsilon_0$ (table 1). The numerical vertical velocity field $w(x,z,t)$ of the pycnocline layer $z \in [z_1 = -h_1,\ z_2 = -h_2]$ is then projected on each analytical vertical modal structure $W_n(z)$. A fixed time-space window has been defined above the flat bottom and close to the generation site to minimize dissipation effects on vertical mode amplitude: $x \in [x_1 = 0.97\ m > l + A\ ,\ x_2 = 1.55\ m]$). This space window is referred as the "near field" area on Figure 1. The time window contains two tidal periods and starts when the transitory period of mode 4 is over inside the near field area: $t \in \left[t_1 = 80s \geq \frac{x_2}{c_4}, t_2 = 2T + t_1 = 112\ s \right]$. For each resulting projection $(P_{n,w}(x,t))$, we calculate the residual signal $(w(x,z,t) - \sum_{i=1}^{n-1} P_{i,w}(x,t) \cdot W_i(z))$ before applying the next vertical mode projection:

$$P_{n,w}(x,t) = \langle w(x,z,t) - \sum_{i=1}^{n-1} P_{i,w}(x,t) \cdot W_i(z), W_n(z) \rangle \qquad (4)$$

where $\langle\ ,\ \rangle$ indicates a scalar product. Frequency spectra were calculated on $P_{n,w}(x,t)$ by a fast Fourier transform at each point in space. In our configurations, there is only one tidal frequency but tidal harmonics can be generated. Moreover, non-linearity can induce the emerging of additional characteristic frequencies on the frequency spectra (Mercier *et al.*[16], Dossmann *et al.*[17]). The amplitude of the spectrum at the fundamental frequency ($f_0 = 1/T = 0.0625\ s^{-1}$) is considered as the amplitude of the vertical mode: $A_{n,w}(x) = P_{n,w}(x, f_0)$. Figure 2 represents the spatial average of vertical mode amplitudes over the "near field" area (shaded area on Figure 1) for 12 simulations representing a wide range of topography widths: $\lambda_r \in [0.2 - 2]$ m. This figure illustrates the influence of the topography width on tidal energy distribution among vertical modes.

Influence of the topography width λ_r : a resonance phenomenon

As highlighted in previous analytical studies of IW generation above small or infinitesimal bottom topography[5,7], there is, in our specific configuration, a resonance phenomenon between the vertical mode wavelength and the topography width. Indeed the relation between vertical mode amplitude and topography width is not linear: vertical mode amplitude presents a maximum for a narrow range of topography width. The amplitude of each mode n is maximal when the topography width λ_r is of the same order as its wavelength λ_n: $\frac{\lambda_n}{\lambda_r} \approx 1$ (area indicated by colored patch, clearly visible for mode 2 and 3). As a consequence, high mode amplitude increases with narrower and steeper topography and vanishes for wide topographies. This resonance phenomenon can be related to an energy

ACCEPTED MANUSCRIPT

AIP Publishing

This manuscript was accepted by Phys. Fluids. Click here to see the version of record.

exchange with the tidal current. Vlasenko and Stashchuk[18] highlight a mechanism of suppression or amplification of internal waves by a current over an inclined bottom. They showed, in particular, that internal waves gain energy when they propagate downslope–downstream and lose energy when they propagate downslope–upstream. Hence, the amplitude of a vertical mode *n* must be maximal when it propagates, away from the ridge, downslope-downstream (amplification), and is no longer above the varying topography area (out of the generation site) when the tidal current reverses (in this way , the mode *n* does not propagate downslope-upstream and so there is no suppression). When the distance d_n, travelled in *T/2* time interval, is superior to the half-width of the topographic obstacle, mode *n* amplitude is amplified by energy exchange with tidal current: $d_n(T/2) = c_n T/2 \geq \lambda_r/2 <=> \lambda_n \geq \lambda_r$. Moreover, when the resonance criterion is met ($\lambda_n = \lambda_r$), the time interval during which mode *n* propagates downslope-upstream is maximal and thus the amplification effect by tidal current is maximal.

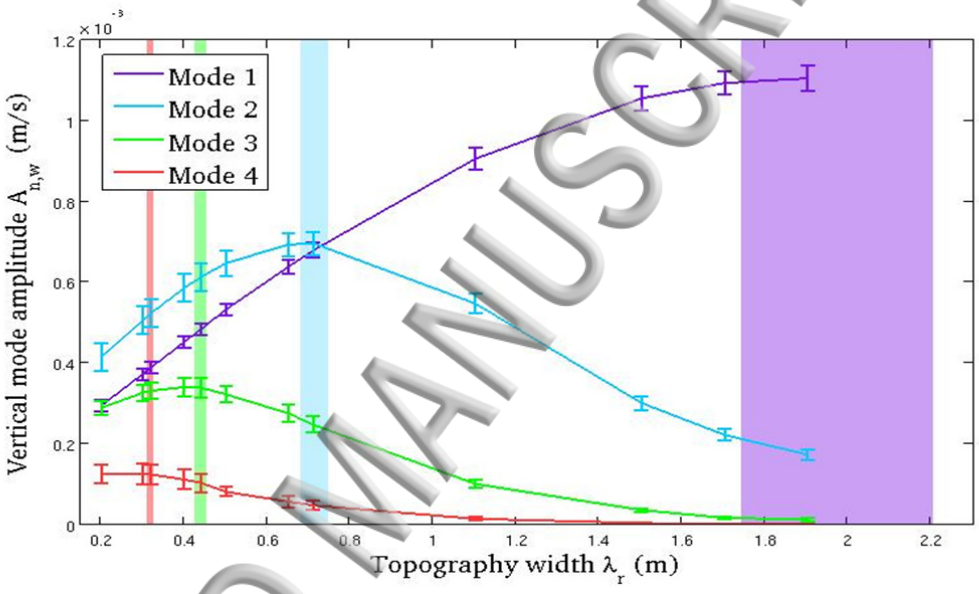

FIG. 2. Spatial average of vertical mode amplitudes over the "near field" area versus the width λ_r of the ridge for a fixed ridge height (h_0=0.07m). Each colored line represents one vertical mode (n=1..4). The confidence intervals are defined using twice the standard deviation of the vertical mode amplitude inside the "near field" area. Each colored patch represents an analytical estimate of the associated vertical mode wavelength, λ_n above the ridge. The maximal value is estimated by resolving the classical Sturm-Liouville eigenvalue problem of vertical mode decomposition above the flat bottom i.e. from the complete stratification profile: *N(z=[-H,0])*. The minimal value is estimated from the stratification profile at the ridge top: *N(z=[-h₀,0])*. λ_n refers to an average value between these two extremes in order to take account of the ridge height effect.

Tidal energy distribution among vertical modes at fixed topography width

Previous analytical studies[5,7] show that for a constant topography width and above small or infinitesimal sinusoidal topography, vertical mode amplitude a_n decreases with the mode number *n*. In fact, according to the data of many field observations, in the ocean, the first mode usually dominates. However, in our configurations, above narrow and abrupt topography (small λ_r), lowest modes are not always dominant in the near field area. For example, Mode 2 is the dominant structure in the near field when $\frac{\lambda_2}{\lambda_r} \geq 1$ (figure 2). Moreover, if we estimate the local amplitude of mode 3 at the base of the ridge ($x \in [l + A, x_1]$), it is also larger than mode 1 amplitude, $A_{3,w} > A_{1,w}$, when $\frac{\lambda_3}{\lambda_r} \geq 1$ (not shown). Mode 3 is suspected to be the dominant structure for narrower topography. However, when

ACCEPTED MANUSCRIPT

AIP Publishing

This manuscript was accepted by Phys. Fluids. Click here to see the version of record.

the topography width is inferior to 0.1167, nonlinearities and secondary peaks appear on the frequency spectrum ($\varepsilon \geq \varepsilon_0$). Then the base projection (the modal vertical structures) may not be appropriate anymore.

To summarize, in our particular configuration of high topography with non-uniform stratification, mode amplitude, a_n, for fixed values of topography width λ_r, does not decrease necessarily with n. Indeed, for narrow topography, mode 1 is no longer the most energetic one. Similarly, Falahat et al.[6] calculated analytically tidal energy conversion into vertical normal modes in the case of a unidirectional tide impinging on a Witch of Agnesi ridge for three different stratification profiles. For stratification profiles with a strong pycnocline layer, mode 1 was the most energetic mode only for wide ridge whereas for constant stratification profile mode 1 was almost always the most energetic one.

Influence of the topography height h_0

It is established that the topography height (h_0) can also influence the tidal energy distribution between vertical modes[5]. Three simulations with different topography heights: $h_0 = [0.03; 0.04; 0.07]\ m$, are now investigated with mode 2 resonance condition ($\frac{\lambda_2}{\lambda_r} \approx 1$). The blocking parameter ($B = h_0/h_2$) describes the interaction degree between the topography and the pycnocline layer. The more intense the topographic blocking effect ($B \rightarrow 1$), the higher the energy distribution in higher modes (Table 2). For small blocking parameters, B = 0,3-0,4, mode 1 is the dominant structure inside the pycnocline layer all over the domain ($A_{n,w} < A_{1,w}$) whereas for higher blocking parameter, B = 0.7, mode 2 is becoming the dominant vertical structure near the generation site ($A_{2,w} > A_{1,w}$). Similarly, Vlasenko et *al.* calculated vertical mode amplitude above continental shelves. They found that the decrease in efficiency of the generation of high modes was accompanied by an increase of the depth of the continental shelves. Hence, we can confirm that narrow and shallow topographic obstacles are identified as efficient generation site of high modes.

	B=0.3	*B=0.4*	*B=0.7*
$A_{1,w}$ $(\times 10^{-4}\ m/s)$	**2.3** ∓ 0.08	**3.3** ∓ 0.1	7.2 ∓ 0.3
$A_{2,w}$ $(\times 10^{-4}\ m/s)$	2.2 ∓ 0.05	3.2 ∓ 0.08	**7.6** ∓ 0.3
$A_{3,w}$ $(\times 10^{-4}\ m/s)$	0.6 ∓ 0.04	1.1 ∓ 0.06	3.3 ∓ 0.3
$A_{4,w}$ $(\times 10^{-4}\ m/s)$	0.05 ∓ 0.02	0.1 ∓ 0.04	0.9 ∓ 0.2

TABLE 2 - Spatial average of vertical mode amplitudes over the "near field" area $A_{n,w,}$ in function of the blocking parameter B in the case of mode 2 resonance condition: $\lambda_r \approx \lambda_2$. The confidence intervals (indicated in grey) are defined using twice the standard deviation of the vertical mode amplitude inside the "near field" area.

Conclusion

In summary, we provide a numerical estimate of the tidal energy distribution among vertical modes in highly energetic generation sites: strong pycnocline layers above high and abrupt sinusoidal topographies. The distribution of the conversion energy over different vertical modes is important to evaluate precisely the spatial redistribution of the tidal energy. We developed a method to quantify vertical normal mode amplitude in 2D direct numerical simulations. Our numerical study highlights a topographic resonance phenomenon on vertical mode generation consistent with previous analytical studies[5,7]. To characterize this resonant effect, we define a topographic resonance criterion: mode n has maximal amplitude when its wavelength λ_n is of the same order than the topography width λ_r: $\frac{\lambda_n}{\lambda_r} = 1$. This resonance phenomenon is linked to energy exchanges with tidal flow. In our particular configuration, near the generation site, vertical mode amplitude a_n does not always decrease with the mode

ACCEPTED MANUSCRIPT

AIP Publishing

This manuscript was accepted by Phys. Fluids. Click here to see the version of record.

number n. For wide or small topographies (B<1), mode 1 is the most energetic mode whereas for narrow and high topographies ($B\rightarrow1$) mode 2 and 3 are more energetic than mode 1. Hence, the tidal energy distribution among vertical mode is shown to be dependent on the topographic resonance criterion ($\frac{\lambda_n}{\lambda_r}=1$) and on the topographic blocking parameter $B = h_0/h_2$. In the linear regime, shallow ($B\rightarrow1$) and narrow ridges (selecting small λ_n) are identified as generation sites effective at generating high vertical modes. These two criteria could be used to differentiate efficient radiative generation sites (tidal energy is mostly injected in mode 1) from generation sites where tidal energy is more likely to dissipate locally (tidal energy is injected in higher modes). These results are a step towards future work on the horizontal distribution of the diapycnal mixing. In future studies, it would be of interest to investigate more deeply tidal energy distribution among vertical normal modes in the non-linear regime.

[1] W. Munk and C. Wunsch, "Abyssal Recipes II: Energetics of Tidal and Wind Mixing", Deep Sea Res. Part Oceanogr. Res. Pap. **45**, 1977–2010 (1998).
[2] G.D. Egbert and R.D. Ray, "Significant Dissipation of Tidal Energy in the Deep Ocean Inferred from Satellite Altimeter Data", Nature **405**, 775–778 (2000).
[3] C. Wunsch and R. Ferrari, "Vertical Mixing, Energy, and the General Circulation of the Oceans", Annu. Rev. Fluid Mech. **36**, 281–314 (2004).
[4] R. Ferrari and C. Wunsch, "Ocean Circulation Kinetic Energy: Reservoirs, Sources, and Sinks", Annu. Rev. Fluid Mech. **41**, 253–282 (2009).
[5] V. Vlasenko, N. Stashchuk, and K. Hutter, "Baroclinic Tides: Theoretical Modeling and Observational Evidence" (Cambridge University Press, 2005).
[6] S. Falahat, J. Nycander, F. Roquet, and M. Zarroug, "Global Calculation of Tidal Energy Conversion into Vertical Normal Modes", J. Phys. Oceanogr. **44**, 3225–3244 (2014).
[7] T. Gerkema and J.T.F. Zimmerman, "An Introduction to Internal Waves: Lecture Notes", R. NIOZ(2008).
[8] Y. Dossmann, F. Auclair, and A. Paci, "Topographically Induced Internal Solitary Waves in a Pycnocline: Primary Generation and Topographic Control", Phys. Fluids **25**, 66601 (2013).
[9] F. Auclair, C. Estournel, J.W. Floor, M. Herrmann, C. Nguyen, and P. Marsaleix, "A Non-Hydrostatic Algorithm for Free-Surface Ocean Modelling", Ocean Model. **36**, 49–70 (2011).
[10] F. Auclair, L. Bordois, Y. Dossmann, T. Duhaut, A. Paci, C. Ulses, and C. Nguyen, "A Non-Hydrostatic Non-Boussinesq Algorithm for Free-Surface Ocean Modelling", Ocean Model., (First submission 2014).
[11] Y. Dossmann, F. Auclair, and A. Paci, "Topographically Induced Internal Solitary Waves in a Pycnocline: Secondary Generation and Selection Criteria", Phys. Fluids **25**, 86603 (2013).
[12] Y. Dossmann, Ondes internes générées sur une dorsale océanique: du laboratoire à l'océan, phdthesis, Université Paul Sabatier - Toulouse III, 2012.
[13] F. Auclair, L. Bordois, Y. Dossmann, T. Duhaut, C. Estournel, J.W. Floor, P. Marsaleix, C. Nguyen, A. Paci, and C. Ulses, "Implementation of a Time-Dependent Bathymetry in a Free-Surface Ocean Model: Application to Internal Wave Generation", Ocean Model. **80**, 1–9 (2014).
[14] T. Gerkema and J.T.F. Zimmerman, "Generation of Nonlinear Internal Tides and Solitary Waves", J. Phys. Oceanogr. **25**, 1081–1094 (1995).
[15] N. Grisouard, C. Staquet, and T. Gerkema, "Generation of Internal Solitary Waves in a Pycnocline by an Internal Wave Beam: A Numerical Study", J. Fluid Mech. **676**, 491–513 (2011).
[16] M.J. Mercier, L. Gostiaux, K. Helfrich, J. Sommeria, S. Viboud, H. Didelle, S.J. Ghaemsaidi, T. Dauxois, and T. Peacock, "Large-Scale, Realistic Laboratory Modeling of M2 Internal Tide Generation at the Luzon Strait", Geophys. Res. Lett. **40**, 5704–5709 (2013).
[17] Y. Dossmann, A. Paci, F. Auclair, M. Lepilliez, and E. Cid, "Topographically Induced Internal Solitary Waves in a Pycnocline: Ultrasonic Probes and Stereo-Correlation Measurements", Phys. Fluids **26**, 56601 (2014).
[18] V. Vlasenko and N. Stashchuk, "Amplification and Suppression of Internal Waves by Tides over Variable Bottom Topography", J. Phys. Oceanogr. **36**, 1959–1973 (2006).

ACCEPTED MANUSCRIPT

ACCEPTED MA

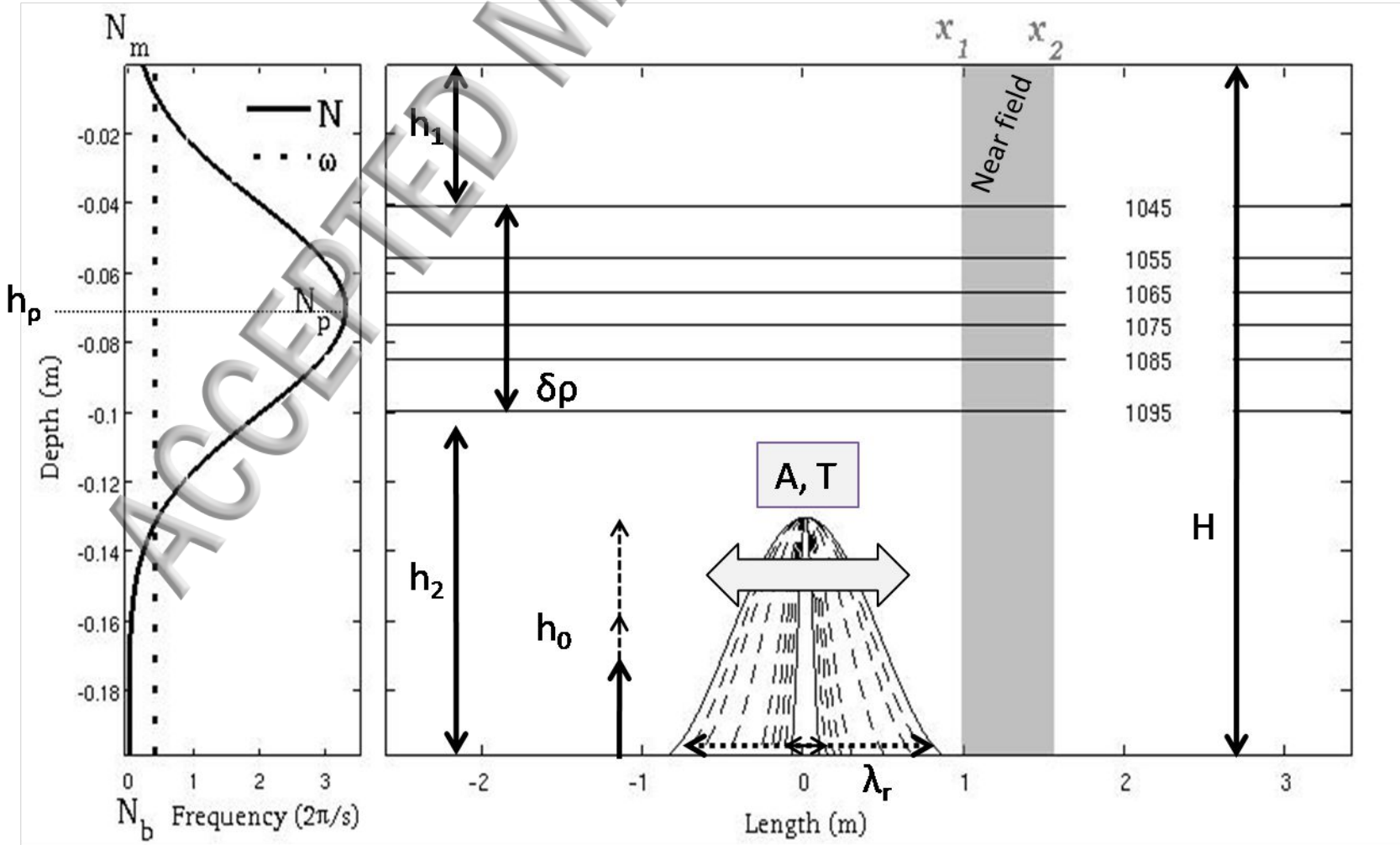
N_m
N
ω
h_p
N_p
Depth (m)
-0.02
-0.04
-0.06
-0.08
-0.1
-0.12
-0.14
-0.16
-0.18
0
1
2
3
N_b Frequency (2π/s)
x_1
x_2
Near field
h_1
δρ
h_2
h_0
A, T
λ_r
H
1045
1055
1065
1075
1085
1095
-2
-1
0
1
2
3
Length (m)

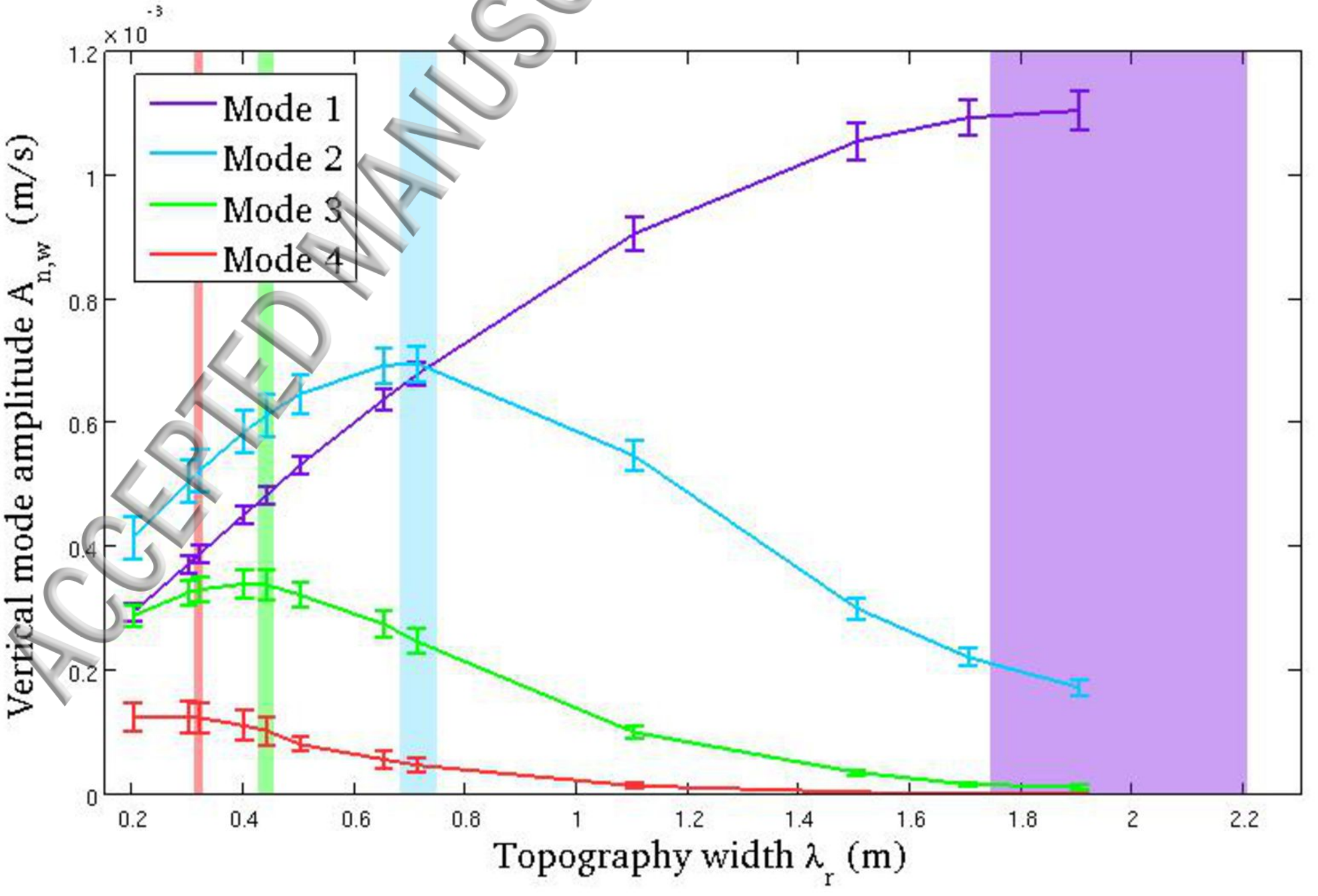

ACCEPTED MANUSCRIPT